Photogrammetria, 32 (1976) 75—100

IMAGING RADAR APPLICATIONS TO MAPPING AND CHARTING*

FRANZ LEBERL

Resident Research Associate of the U.S. National Academy of Sciences, National Research Council, Jet Propulsion Laboratory, California Institute of Technology, Pasadena, Calif. 91103 (U.S.A.)

(Received August 20, 1976)

ABSTRACT

Leberl, F., 1976. Imaging radar applications to mapping and charting. Photogrammetria, 32: 75—100.

The present paper will review past and present radar mapping achievements and examine tasks and prospects of radargrammetry. The radar mosaic at scales 1:100,000 to 1:400,000 is thus far the typical radar mapping product applied to vast areas in excess of 10 million square kilometers, mainly in Latin America, the U.S., Indonesia, the Philippines and Australia. During the past several years it has been learned that aircraft radar permits mappir of extensive areas with a planimetric accuracy of about 100 m, and in exceptional cases, of about 20 m. For stereo-radargrammetric height accuracy, also about 20 m was found to be feasible. Radar mapping has presently become possible from spacecraft. Up to now, orbital radar images have only been produced for lunar exploration. An earth resources imaging satellite radar will orbit our planet as part of the SEASAT experiment from 1978 onwards. It is thus possible that radar images might in the future be applied to a dramatically greater extent than in the past to mapping tasks for which timeliness and economy are of overriding concern.

INTRODUCTION

The period since 1972 was marked by a steady increase in the use of SLR imagery particularly for reconnaissance-type mapping at small scales (1:100,00(and smaller). Military security restrictions on radar resolution, and on radar studies, were largely dropped, so that at present radar data are available for civilian purposes with a ground resolution of up to 3×3 m^2. The advent of orbital SLR also fell in the period since 1972. Further momentum has been gained by geo-science SLR due to increased efforts by the U.S. National Aeronautics and Space Administration (NASA) to prepare for earth-orbiting satellite radars becoming available in the near future.

Radargrammetric studies have been performed addressing all three of the basic units of photogrammetry, namely the single image, the single stereo mode and the block of overlapping imagery. However, many studies concentrated on the single image. The intensity of work was less for stereo analysis and least in block-adjustment. Most of these studies could be based on actually available

*Invited paper, Commission III, 13th Congress of the International Society for Photogrammetry, Helsinki, 1976.

radar imagery. The pre-1972 tendency persisted, however, to employ only very small samples of real data and to study them in an environment and under assumptions that are remote from a production situation.

The present paper attempts to outline the major actual and potential radar mapping applications, to give an account of the present state of satellite radar imaging, and review the radargrammetric work that has been performed since 1972. This review will address separately the single radar image, the radar stereo model and the radar block.

RADAR MAPPING APPLICATIONS

Actual applications

By far the most prominent operational imaging radar application is planimetric reconnaissance-type mapping of cloud-infested remote areas at scales of 1:100,000 and smaller. Vast areas of the world have been mapped in this way; the majority of these efforts have taken place since 1972. Although Brazil had begun its extensive Radar Mapping of the Amazon — RADAM — in 1971 (De Azevedo, 1971; Moreira, 1973), it only recently (and in spite of available LANDSAT-MSS coverage) completed the acquisition of images of its entire territory of 9 million km^2. All Latin-American countries sharing the Amazon Basin have now obtained radar coverage of this area. In addition, Peru mapped a large portion of the Andes by radar, Colombia its Pacific Coast and Nicaragua its entire territory. Other mapping projects include portions of the Philippines, Indonesia, New Guinea and Australia. On most of these projects, there exists no generally available published documentation.

Projects with a near-operational character and a radargrammetric element concerned the application of radar to the mapping of lake ice distribution (Schertler et al., 1975) and to the tracking of icebergs (Super et al., 1975). Sea ice mapping with radar seems only to have been developed to a near-operational status in the U.S.S.R. (Glushkov et al., 1972).

A series of other operational radar applications has thus far not employed radargrammetric techniques. It seems that radar images are being acquired by oil and mineral exploration companies for the study of regional geological fracture patterns and stream network analysis and for the selection of sites for dams and nuclear power plants. However, the compilation of image mosaics is generally without control.

Potential applications

Radar has potential applications in a number of geoscience fields, for which radargrammetry would be at least as much a supporting tool as photogrammetry presently is in the use of metric photography. A major radargrammetric element would occur if future potential applications required the merging of image data from various sensors and times. Attempts to merge data from different sensors

are presently being undertaken (Harris and Graham, 1976). No specific conclusions have been reached as to a geoscience application of such techniques. However, there seems to be a growing awareness among remote-sensing specialists that (1) ultimately remote-sensor data from many sources have to be combined for optimum interpretability; (2) the detection of changes from sequential imagery will have to consider thoroughly metric aspects of the images; and (3) the topography of the mapped terrain is of such importance to the energy—matter interaction that the (digital) terrain model (DTM) might ultimately find a remote-sensing application in addition to its mapping and civil engineering application.

Radar could be of potential use in the revision of small-scale maps. At the present time this potential is, however, entirely unexplored.

A potentially major future task, particularly of satellite radar, may consist of mapping the polar ice motion (ice dynamics). Although charting the distribution of icebergs, lake and sea ice (Fig. 1) for ship navigation has reached a near-operational status, mapping of the motion of the polar ice still requires considerable efforts (Leberl et al., 1976a).

SATELLITE RADAR

The first satellite radar images were produced in the Apollo Lunar Sounder Experiment (ALSE) during the Apollo 17 mission to the moon (Phillipps et al., 1973); an example is shown in Fig. 2. Radargrammetric studies were carried out with single images (Tiernan et al., 1976), and with a stereo model (Leberl, 1975e, 1976a).

The first earth-orbiting satellite to carry an imaging radar system will be SEASAT, scheduled for launch in 1978. Its main purpose will be to image the oceans, polar ice and coastal areas of North America. Unlike LANDSAT, it will not be aimed at imaging the entire world. The image data will be received through modified LANDSAT-ground stations. The additional equipment to do so will require sizeable expenditures. However, the U.S. National Aeronautic and Space Administration (NASA) might be in a position to have portable versions of the SEASAT radar receiving equipment made available temporarily.

Other satellite imaging-radar projects, which at present are only in a planning

Fig. 1. Side-looking radar image of Arctic sea ice. Arctic ice floes imaged on 18 August 1976 by JPL's L-band synthetic aperture radar system; images were taken during a mission for the Arctic Ice Dynamics Joint Experiment (AIDJEX). Scale: 3 km

stage, concern the exploration of the planet Venus (Rose and Friedman, 1974) and multifrequency radar images of the earth to be produced on board the Space Shuttle (Cohen et al., 1975).

Table I summarizes those parameters of the SEASAT imaging radar that are of radargrammetric relevance. Differences between airborne and satellite imaging radar do not concern the principle of operation of the sensor, nor are there differences in resolution, swath width or scale. Essential differences relat only to the "look-angles" or elevation angles of the line of sight, consideration of the planetary curvature and various effects of orbit parameters. With airborne radar, elevation angles are normally rather large and vary greatly within a swath, e.g., from 40° (near range) to 80° (far range). In a satellite radar at a great orbital altitude, the horizon and energy requirements limit the elevation angles to comparatively small values, and the variation of the angles from near to far range is rather small (see for example SEASAT, Table I). This permits image acquisition under almost constant look angles as opposed to airborne radar, and might enhance the value of the resulting imagery for geoscience applications.

REVIEW OF PROJECTION EQUATIONS FOR REAL- AND SYNTHETIC-APERTURE RADAR

The basic radar imaging and projection equations have been derived on many occasions in the past (for example: Konecny and Derenyi, 1966; Akowetzki, 1968; Derenyi, 1970; Gracie et al., 1970; Leberl, 1970; Hockeborn, 1971; Norvelle, 1972; Greve and Cooney, 1974; DBA-Systems, 1974). They were

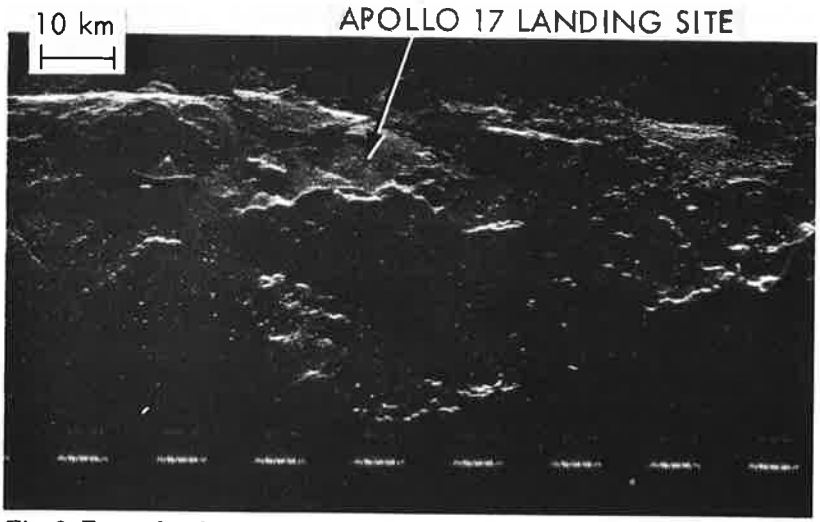

Fig. 2. Example of orbital side-looking radar image produced during the Apollo-17 mission to the moon. Image taken with ALSE-VHF (2 m wavelength) synthetic aperture radar.

TABLE I

Radargrammetrically relevant parameters of the SEASAT-satellite imaging radar system

Launch	May 1978 (scheduled)
Orbit altitude	790 - 820 km
Orbit inclination	108° retrograde
Orbit period	100 minutes
Radar wavelength	25 cm (L-band)
Elevation angles of line of sight	16.9° - 23.1°
Swath width	100 km
Resolution along track	7 m (25 m)*
Resolution across track in slant range	8 m
in ground range	25 m
Dynamic range	50 db
Transmitted radar image data received by modified LANDSAT stations	
Recording of received data probably on magnetic tape	
Map film generation by optical or digital correlation	

*The 7 m resolution will in most radar presentations be artificially degraded to 25 m to achieve equal resolution along and across track and to smooth the graininess of the original data (multi-look mode of presentation)

well-established prior to 1972. However, it might be of value to specifically review the differences which exist in the projection equations for radar with real and with synthetic aperture; synthetic-aperture radars have become of growing importance during the last few years and are the only system to be made use of from satellites.

Irrespective of the type of side-looking radar imagery, the basic measurement to work with is the slant range r_p between the antenna and point P, and time of imaging, t_p. These entities are obtained in a simple process from measurements in the photographic radar record (see for example, Konecny and Derenyi 1966; Rydstrom, 1968; Leberl, 1972a). The basic radargrammetric difference between real and synthetic-aperture radar is the following: for real apertures, all points imaged at time t lie on a surface whose orientation is defined by the

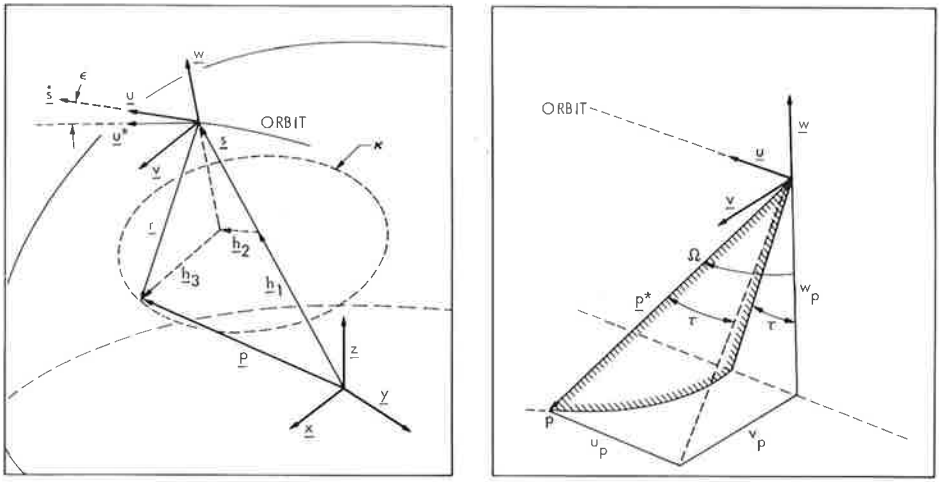

Fig. 3. Coordinate system and definitions for radar projection equations. a. Planetocentric and antenna systems, K = intersection of range sphere and planetary surface (reference figure). b. Cone complement angle, τ and vector **p***.

attitude of the real antenna; for synthetic apertures, the orientation of the imaging surface is determined by the *velocity vector of the real antenna.*

The position of the radar sensor is denoted by a vector* $\mathbf{s}(t) = [x_s(t), y_s(t), z_s(t)]$. The sensor position is a function of time t. The velocity vector of the antenna is the first derivative of $\mathbf{s}(t)$ with respect to time t and denoted by $\dot{\mathbf{s}}(t) = [\dot{x}_s(t), \dot{y}_s(t), \dot{z}_s(t)]$. The antenna attitude, finally, is determined by the three classical orientation angles of photogrammetry: $\phi(t)$, $\omega(t)$, $\kappa(t)$. In the following, the time dependency will not be explicitly indicated, so that $\mathbf{s}=\mathbf{s}(t)$, etc.

A formulation for the projection equation of side-looking radar is now (Fig. 3a, b):

$$\begin{aligned} \mathbf{p} &= \mathbf{s} + \mathbf{r} \\ \mathbf{r} &= u_p\mathbf{u} + v_p\mathbf{v} + w_p\mathbf{w} \end{aligned} \qquad (1)$$

where **p** is the position vector of an imaged point in object space; **u**, **v** and **w** are unit vectors defining the rectangular antenna coordinate system; **r** is the range vector from the antenna to the object point; and the auxiliary vector $\mathbf{p}^* = (u_p, v_p, w_p)$ describes the location of the object point in the **u**, **v**, **w** antenna coordinate system (see Fig. 3b):

$$\begin{aligned} u_p &= r \sin\tau \\ v_p &= (\sin^2\Omega - \sin^2\tau)^{1/2}\, r \\ w_p &= -\cos\Omega\; r \end{aligned} \qquad (2)$$

*Vectors are denoted by bold-faced, lower-case letters. The dot product is denoted by (•), and the crossproduct by (×). Matrices are denoted by bold-faced capitals.

where τ is the "cone-complement angle". Hockeborn (1971) calls τ "squint"; it is also explained by Graham (1975a), Leberl (1972a,b; 1975a,b) and discussed in considerable detail by Leberl (1976b).

Eq. 1 can be rewritten in a more familiar form as:

$$\mathbf{p} = \mathbf{s} + \mathbf{A}\,\mathbf{p}^{\star} \tag{3}$$

where the rotation matrix A describes the rotation of vectors **u**, **v**, **w** parallel to **x**, **y**, **z**, so that:

$$\mathbf{A} = \begin{bmatrix} x_u\, y_u\, z_u \\ x_v\, y_v\, z_v \\ x_w\, y_w\, z_w \end{bmatrix} \tag{4}$$

For a real-aperture radar matrix A contains the orientation angles ϕ, ω, κ, in their familiar form (see, for example, Leberl, 1972a). For synthetic aperture radar, however, vectors **u**, **v** and **w** are functions of the velocity vector $\dot{\mathbf{s}}$ and position vector **s**:

$$\begin{aligned} \mathbf{u} &= \dot{\mathbf{s}}/|\dot{\mathbf{s}}| \\ \mathbf{v} &= (\mathbf{s} \times \dot{\mathbf{s}})/|\mathbf{s} \times \dot{\mathbf{s}}| \\ \mathbf{w} &= (\mathbf{u} \times \mathbf{v})/|\mathbf{u} \times \mathbf{v}| \end{aligned} \tag{5}$$

Eqs. 1 or 3 can now be rewritten in several ways, of which the most common (Konecny, 1970, 1972a; Gracie et al., 1970, 1972; Leberl, 1971c, 1972a, 1972b; Greve and Cooney, 1974; DBA-Systems, 1974) can be given in vector notation as:

$$|\mathbf{p} - \mathbf{s}| = r \tag{6}$$

$$\mathbf{u} \cdot (\mathbf{p} - \mathbf{s}) = \sin\tau\ |\mathbf{u}|\ |\mathbf{p} - \mathbf{s}| \tag{7}$$

Eq. 6 represents a sphere with its center at **s** and radius r ("range-sphere"). Eq. 7 represents a cone with the axis along vector **u** (**u** defines the longitudinal axis of the real antenna; or it defines the direction of the velocity vector **s**, which in turn is the longitudinal axis of the synthetic antenna). If the radar operation is "normal", then $\tau = 0$ and the cone degenerates to a plane (the so-called "scanning plane"):

$$\mathbf{u} \cdot (\mathbf{p} - \mathbf{s}) = 0 \tag{8}$$

For completeness, it should be mentioned that the previous equations neglect the small offset $\Delta\mathbf{s}$ between the sensor platform, whose position is defined by **s**, and the antenna. It might also be worthwhile to point out that the rotation matrix A for real aperture radar might be a composite of several rotations (antenna into antenna mount; antenna mount into sensor platform; sensor platform into reference system).

SINGLE-IMAGE RADAR MAPPING

Mapping with single radar images has been carried out with the objective to derive object coordinates of imaged points either with or without the use of ground control points; to rectify the radar image for enhanced interpretability or for mosaicking; and to produce a line plot as a cartographic product. The following will address first the mathematical methods of single-image radar mapping, and then analyze the accuracy by reviewing the studies that have been carried out on this topic.

Mapping methods

The inputs to single-image radargrammetry consist of (1) the measurements of slant range, r_i, and time of imaging, t_i, of a selected number of image points $p_i (i = 1, \ldots, i_p)$; (2) the measurements of the sensor-position $\mathbf{s}(t_j)$, $(j = 1, \ldots, j_s)$ and sensor velocity $\dot{\mathbf{s}}(t_j)$ or attitude $\phi(t_j)$, $\omega(t_j)$, $\kappa(t_j)$; (3) the position vecto $\mathbf{g}_k$ of a number of ground control points g_k, $(k = 1, \ldots, k_g)$; (4) perhaps a digital terrain model (DTM) of the imaged object.

Computation of the position vector $\mathbf{p}_i$ of a ground point can be based on either eqs. 1 or 6 and 7. The three eqs. 1 contain four unknowns ($\mathbf{p}_i = (x_{pi}, y_{pi}, z_{pi})$ and Ω_{pi}); the alternative formulation of eqs. 6 and 7 consists of two equations with three unknowns (x_{pi}, y_{pi}, z_{pi}). Obviously, one of the unknown has to be externally measured or given so that the equations can be solved.

In single-image radargrammetry, the unknown to be given (or to be assumed to be known) is the height of the object. Two distinct cases can be differentiat (1) the simplified case, with a straight, level flight parallel to the x-coordinate axis; (2) the general case, with measured flight parameters, in a geocentric coordinate system.

The following will discuss these two cases and then present a method of using ground control points; it will treat the rectification of imagery and the merging of the radar image with digital height data in a process of "digital mono-plotting."

Simplified case of coordinate computation. Often a simplified flight configuration is assumed for single-image radargrammetry (e.g. Rydstrom, 1968; Moore, 1969; Bosman et al., 1971, 1972a,b; Koopmans, 1974; Hirsch et al., 1976). With a straight, level, and undisturbed flight parallel to the x-coordinate axis, the inputs to equations 1 or 3 simplify to:

$$\mathbf{s} = (x_s, 0, h) \qquad \dot{\mathbf{s}} = (|\dot{\mathbf{s}}|, 0, 0)$$

$$\phi = \kappa = 0 \qquad \tau = 0$$

so that:

$$\begin{aligned} x_p &= x_s \\ y_p &= [r^2 - (h - z_p)^2]^{1/2} \\ z_p &= z_p \end{aligned} \tag{9}$$

General case of coordinate computation. The position of the sensor is measured by an inertial or similar guidance system, by SHORAN or HIRAN tracking, or by satellite orbit determination. In all these cases it is convenient to work in a geo-(planeto-) centric coordinate system. The height of the object is in this case expressed as the radius R of the refernece spheroid or sphere. According to Leberl (1975e) one obtains from Fig. 3:

$$\mathbf{p} = \mathbf{h}_1 + \mathbf{h}_2 + \mathbf{h}_3 \tag{10}$$

where (note that $R = |\mathbf{p}|$):

$$h_1 = (|\mathbf{p}|^2 + |\mathbf{s}|^2 - r^2)/(2\ |\mathbf{s}|)$$

$$\mathbf{h}_1 = h_1\ \mathbf{s}/\ |\mathbf{s}|$$

$$\mathbf{u}^{\star} = \mathbf{v} \times \mathbf{s}/|\mathbf{v} \times \mathbf{s}| \text{ (for v, see eq. 5)}$$

$$\cos \epsilon = \mathbf{u}^{\star} \cdot \dot{\mathbf{s}}/\ |\dot{\mathbf{s}}|$$

$$\mathbf{h}_2 = \mathbf{u}^{\star}[(|\mathbf{s}| - h_1) \tan \epsilon + r \sin\tau]$$

$$g = (|\mathbf{s}| - h_1)^2$$

$$\mathbf{h}_3 = \mathbf{v}\ (r^2 - |\mathbf{h}_2|^2 - g)^{1/2}$$

Ground control points. Ground control points can be used in one of two ways: (1) interpolatively; (2) parametrically. In the interpolative method, the radargrammetrically computed position vectors $\mathbf{p}_k$ and the given ground points $\mathbf{g}_k$ define difference vectors $\Delta\mathbf{p}_k$ ($k = 1, \ldots, k_g$). These can be used to interpolate

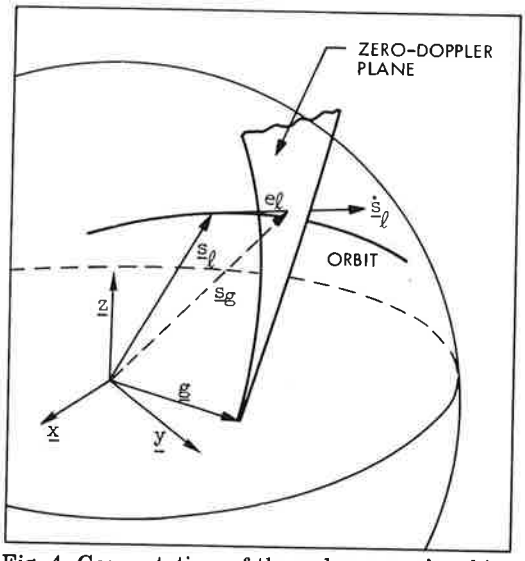

Fig. 4. Computation of the radar sensor's orbit position from where ground point g was imaged (single image radar resection).

corrections in radargrammetric points. Leberl (1971c, 1972a) evaluated a series of different interpolation algorithms with the result that piece-wise polynomials performed best; and Derenyi (1974a) experimentally searched for the optimum polynomial.

An elegant parametric method of using ground control points was formulat by Gracie et al. (1970, 1972) and used by Greve and Cooney (1974) and Leberl (1975e). This method applies to synthetic-aperture radar. According to Fig. 4, a plane through the ground point g, but normal to the flight line, is intersected by the flight line. This is represented as a polygon of linear pieces carrying an index $l (l = 1, \ldots, l_s)$:

$$e_l = \dot{\mathbf{s}}_l \cdot (\mathbf{s}_l - g) \tag{11}$$

$$\mathbf{s}_g = \mathbf{s}_l + \dot{\mathbf{s}}_l \, e_l \; / \; |\dot{\mathbf{s}}_l| \tag{12}$$

From position vector $\mathbf{s}_g$, the slant range r_g and time of imaging t_g can easily be determined. The radar image also provides an independent measurement of slant range and time, namely r_p, t_p. The discrepancies $\Delta r = r_p - r_g$ and $\Delta t = t_p - t_g$ can define the coefficients of a correction polynomial for the range and time measurements in the radar image.

Rectification. The along-track and across-track coordinates of radar images are generated independently of each other. There is, therefore, the possibility of inconsistencies in along- and across-track scales. In the case of synthetic aperture radar images these inconsistencies can, if known, be removed in the process of converting the raw sensor output (the "signal-histories") into the "map film." The method employs a variable scale setting in the optical correlator (Jensen, 1975; Petersen, 1976). However, there are many more image deformations possible than just those due to a differential scale. Possible sources of such deformations were described by Leberl (1972a), and Van Roessel and de Godoy (1974). Methods of rectification are numerical-graphical (Hockeborn, 1971); electro-optical (diCarlo et al., 1968, 1971; Yoritomo, 1972; Masry et al., 1976), or purely digital (Thompson et al., 1972 Leberl et al., 1976a). Other possible concepts have not been realized.

For the *numerical-graphical* method, an ordered set of image-points ("tick-marks") is first transformed into a map system. Square-shaped image patches are then rectified graphically using the four surrounding tick-marks and an anamorphic viewer as described by Ambrose (1967).

The *electro-optical* method uses a set of ground control points to compute the empirical relationship between the raw and rectified image. The settings of an electro-optical differential rectifier (Gestalt, Radar Restitutor) are then calculated and the radar image is rectified. In the purely *digital* approach, the radar image is digitized and rectified in a digital image processing routine, using knowledge about systematic corrections and a set of ground control points to determine the coefficients of a "rubbersheet" stretch of the radar image.

Single image plotting (digital monoplotting). The method of digital monoplotting is very recent in photogrammetry and has been described and developed for the first time by the Rome Air Development Center (Hall, 1973). It was independently proposed by Makarovic (1973). In this method, relevant image points and lines are digitized off a single image and these digitized data are transformed into a map system using the orientation data of the sensor as well as a digital terrain model (DTM). This method of plotting has been applied to radar imagery by Raytheon (1973) in an operational computer program system (Greve and Cooney, 1974). The program intersects each radar projection circle (eqs. 6 and 7) with the digital terrain surface. This leads to an iterative solution of a nonlinear set of equations.

Mapping accuracy

A large number of studies have addressed the question of how accurately the planimetric coordinates of a point can be determined from a single radar image. Generally, those studies rely on the simplified mathematical model of eq. 9 and subsequent correction of the results using ground control points. Table II summarizes the radargrammetric accuracies obtained by many different authors employing different radar data. The mere listing of these results can lead to wrong conclusions. Some further specifications are, therefore, in place.

Single-image radar mapping is based on assumptions for the surface relief: normally, it is taken to be flat, so that errors occur in those cases where this assumption is not entirely correct. According to eq. 9, such an error Δz_p propagates into the planimetric cross-track coordinate y_p. Similarly, erroneous slant ranges (Δr) create errors in y_p. One finds:

$$\Delta y_p = (r\,\Delta r - h\,\Delta h)/y_p \tag{13}$$

so that for standard deviations σ_r and σ_h:

$$\sigma_y^2 = \frac{r^2}{y^2}\,\sigma_r^2 + \frac{h^2}{y^2}\,\sigma_h^2 = \frac{\sigma_r^2}{\sin^2\Omega} + \frac{\sigma_h^2}{\tan^2\Omega} \tag{14}$$

Eq. 14 clearly shows how the across-track error reduces for increasing look angles Ω, but increases with the errors of range and height.

The results listed in Table II are thus not comparable if they are obtained from imagery taken under different look angles, of terrain with different relief, using different resolutions, or ground points of different identifiability. The orbital radar (Tiernan, 1976; Leberl, 1975e) and the JPL L-band aircraft radar (Leberl et al., 1976a) both employ very steep look angles (elevation angles in orbital radar: 0—55°) so that errors of y are much larger than with systems using larger elevation angles. Also the identifiability of surface features is far inferior on the Moon, or in the Alaskan tundra, to that of man-made features in well-developed areas, where all other results were obtained.

Two accuracy analyses concern specific cases; they are therefore marked by

TABLE II

Mapping accuracies achieved with single image radargrammetry
Resolution data are mostly not accurate and indicate order of magnitude only
Description of relief mostly not available

SOURCE	YEAR	ACCURACY (Meters) along 1σ	ACCURACY (Meters) across 1σ	RELIEF	CONTROL per 100 km²	RESOLUTION (Ground -) Meters	ANTENNA Stabilized	ANTENNA Type	RADAR System Code	SCALE of Images 1:	AREA Designation / Remarks
Gracie	1970	20	14	Flat	10.0	17	yes	synth.	AN-APQ 102		Atlanta, Georgia
Leberl	1971	50	23	Flat	10.0	30	no	real	EMI (U.K.)	200 000	Netherlands
Bosman	1971	47	60	Flat	10.0	30	no	real	EMI (U.K.)	250 000	Netherlands
Konecny	1972	152	255	Mount.		17	yes	real	Westinghouse	216 000	N.Guinee - Conf. Transformation
Greve*	1974	35				≥3	yes	synth.	TOPO II	100 000	Dig. Monoplotting
Goodyear	1974	38	30	Flat	3.0	12	yes	synth.	GEMS 1000	400 000	Phoenix, Arizona
Derenyi	1974	89	111	Hills	1.1	17	yes	real	Westinghouse	250 000	Washington D.C.
DBA-Systems*	1974	51	26		0.5	3	yes	synth.	AN-ASQ 142	100 000	Radar Interferometer
Konecny	1975	80	79	Flat		12	yes	synth.	GEMS 1000	400 000	Phoenix - Conf. Transformation
Derenyi	1975	30	28	Flat		12	yes	synth.	GEMS 1000	400 000	Phoenix - Control Density not Spec.
Tiernan**	1976	209	257	Flat	0.7	30-150	no	synth.	Apollo 17	1 Mill.	Lunar Satellite
Leberl**	1976	147	233	Flat	0.3	30-150	no	synth.	Apollo 17	1 Mill.	Lunar Satellite
Hirsch	1976	120		Flat	3.0	30	no	real	EMI (U.K.)	100 000	Netherlands
Leberl	1976	140	190	Flat	0.3	25-150	no	synth.	JPL L-Band	500 000	Alaskan Tundra - Sat. Radar Simul.

*Other information besides "radar range" was available.
**Satellite radar.

an asterisk (*). The study by DBA-Systems (1974) reports on the planimetric accuracy employing a single radar image and radar interferometer data (for an explanation of the radar interferometer, see: Manual of Photogrammetry, 1966). However, use of the interferometer provides the elevation angle Ω to

TABLE III

Mapping accuracy from a single radar image and an interferometer measuring depression an
AN-ASQ 142 radar system with 3-m resolution used (see DBA-Systems, 1974)

FLIGHT Data	CONTROL per 100 km²	ACCURACY (Meters) along 1σ	ACCURACY (Meters) across 1σ	ACCURACY (Meters) height 1σ
HIRAN	0.0	66.9	23.3	23.3
HIRAN	0.5	57.8	23.3	19.7
None	0.5	51.8	26.6	19.7

an object point. This permits computation of topographic heights even from single images.

For this case, DBA-Systems (1974) obtains results shown in Table III. It should be mentioned that these results concern geometrically probably the best side-looking radar system ("All Weather Mapping System" with AN/ASQ-142) with well-defined control and check points.

The other study is by Raytheon (1973, see also Greve and Cooney, 1974) and employs a digital terrain model (DTM) for digital monoplotting. Consideration of topographic heights should thus reduce the mapping errors.

As a general conclusion, the achieved accuracies vary from better than the radar resolution to several times the range resolution. However, to achieve the sub-resolution accuracy, a very high control-point density is required (see Gracie et al., 1970), with, at the same time, the absence of any topographic relief.

MAPPING FROM A SINGLE RADAR STEREO MODEL

Far less work has been performed on radar stereo mapping than on single-image radargrammetry. However, the methods of stereo mapping and the order of magnitude of what can be expected have been rather well-established, essentially since the 1972 ISP-Congress.

Mapping methods — mathematical formulations

Radar stereo mapping has limited itself to the purely analytical approach. Only for PPI-radar (non-side-looking) has there ever been the concept for a plotting instrument proposed (Levine, 1963).

Derenyi (1970) and Konecny (1970, 1971) have established that the formation of a stereo model (relative orientation) is not determined for strip imagery This leads to the conclusion that radar stereo models can only be formed if the elements of exterior orientation are known (measured).

Model formation consists, thus, of the solution of two pairs of equations (Eqs. 6 and 7); each pair is obtained from one image of the stereo set, denoted by (′) and (″) (see Leberl, 1972b, 1975e):

$$\left.\begin{aligned} |\mathbf{p}-\mathbf{s}'| &= r';\ u' \cdot (\mathbf{p}-\mathbf{s}') = \sin\tau\ |\mathbf{u}'|\ |\mathbf{p}-\mathbf{s}'| \\ |\mathbf{p}-\mathbf{s}''| &= r'';\ u'' \cdot (\mathbf{p}-\mathbf{s}'') = \sin\tau\ |\mathbf{u}''|\ |\mathbf{p}-\mathbf{s}''| \end{aligned}\right| \quad (15)$$

This is a set of four non-linear equations with three unknowns (x_p, y_p, z_p). Linearization leads to a set of correction equations:

$$\mathbf{C} \cdot \mathbf{v}_1 + \mathbf{D}\Delta\mathbf{p} + \mathbf{f}_1 = 0 \quad (16)$$

where vector $\mathbf{v}_1$, contains the correction to the 14 observations ($\mathbf{s}'$, $\mathbf{s}''$, $\dot{\mathbf{s}}'$, $\dot{\mathbf{s}}''$, r', r''); $\Delta\mathbf{p}$ is the vector of unknowns, $\mathbf{f}_1$ of contradictions; $\mathbf{C}$ and $\mathbf{D}$ are coefficie matrices. Solution of this set of equations follows the rules of the method of least squares.

Instead of directly introducing s, $\dot{s}$ as observations into the projection equation, Gracie et al. (1970, 1972) first computed spline polynomials through all observed values of s, $\dot{s}$. The coefficients of the splines were assumed to be constants. Only the time is observed which serves as the parameter of the spline polynomials. This approach thus reduces the number of observations to four (t', t'', r', r''). A completely rigorous approach would however require also the s, $\dot{s}$ to be considered as observations. Such a formulation is used by DBA-Systems (1974) and is also described by Leberl (1976b).

Instead of eq. 15, one can also equate the two sets of eqs. 3 (Leberl, 1972b, 1975e):

$$\mathbf{s}' + \mathbf{A}' \, (\mathbf{p}^{\star})' - \mathbf{s}'' + \mathbf{A}'' \, (\mathbf{p}^{\star})'' = 0 \qquad (17)$$

This is a set of three equations with the two unknown look angles Ω', Ω''. Linearization leads to:

$$\mathbf{E} \, \Delta \mathbf{\Omega} + \mathbf{f}_2 = \mathbf{v}_2 \qquad (18)$$

This approach minimizes the distance between the homologue projection circle

A simplified approach to the formation of a stereo model assumes again, similar to eq. 9, straight and level parallel flights (Derenyi, 1975a,b; Leberl, 1975e):

$$\mathbf{s}' = (x'_s, 0, h) \qquad \mathbf{s}'' = (x''_s, B, h)$$

so that:

$$\begin{aligned} x_p &= (x'_s + x''_s) \, /2 \\ y_p &= (r''^2 - r'^2 - B^2) \, /2B \\ z_p &= h - [\, \{(r''^2 - (y_p - B)^2 \}^{1/2} + (r'^2 - y_p^2)^{1/2} \,] \, /2 \end{aligned} \qquad (19)$$

When ground control points are available, then there are again the same two possibilities of interpolative or parametric use of these points as in the single-image approach: either the model deformations in control points are used to interpolate corrections in radargrammetric points, or the slant ranges and times of imaging are corrected using eqs. 11, 12.

Mapping methods — stereo configurations

The normal case of stereo-radargrammetry consists of two parallel flight lines on the same side of the imaged area ("same-side stereo"). Other configurations, e.g. parallel flight lines on opposite sides of the imaged area ("opposite-side"), or at right angles ("cross-wise" — See Graham, 1975b) can create great difficulties in visually perceiving a stereoscopic model, to the point that such configurations cannot be employed.

This exhausts the possibilities for synthetic aperture radar. For real-aperture radar, there are still a number of possible stereo configurations, which can be generated along a single flight-line, for example imaging with convergent

scanning planes (imaging with ϕ-tilted antennas, Leberl, 1972a); imaging with two κ-swung vertical scanning planes; or the combination of one κ-swung vertical scanning plane with a scanning cone ($\tau \neq 0$; see Carlson, 1973; Bair and Carlson, 1974, 1975). The latter configuration particularly is claimed to provide for a satisfactory visual stereo-effect.

Mapping accuracy

Theoretical studies into the accuracy of a side-looking radar stereo model have been undertaken by Leberl (1972b, 1976b). Expressions for the deformation of a synthetic aperture stereo model were derived by Leberl (1976b). It is shown that for errors pertaining to image ($'$), one obtains:

$$\begin{aligned}
\Delta x_p &= \frac{\Delta x'_s}{2} + \frac{H \tan \Omega'}{2} \Delta \dot{y}'_s - \frac{H}{2} \Delta \dot{z}'_s \\
\Delta y_p &= \frac{\Delta y'_s}{1 - \cot \Omega' \tan \Omega''} + \frac{\Delta z'_s}{\tan \Omega'' - \tan \Omega'} - \frac{\cos \Omega'' \Delta r'}{\sin (\Omega' - \Omega'')} \\
\Delta z_p &= \frac{\Delta y'_s}{\cot \Omega' - \cot \Omega''} + \frac{\Delta z'_s}{1 - \tan \Omega' \cot \Omega''} + \frac{\sin \Omega'' \Delta r'}{\sin (\Omega' - \Omega'')}
\end{aligned} \qquad (20)$$

Eq. 20 show clearly, that the model coordinate in flight direction (x_p) is deformed mainly due to errors of the velocity vector ($\Delta \dot{y}_s$, $\Delta \dot{z}_s$) and that errors in across-track direction (y_p) and in height (z_p) are only the results of erroneous sensor positions (Δy_s, Δz_s) and of an error of range r.

Fig. 5 gives a graphical representation of Δy_p and Δz_p due to $\Delta r'$ and for specific stereo arrangements. It is obvious that small elevation angles Ω', Ω'' lead to small Δz_p errors, but that they inversely create larger Δy_p errors. The opposite is true for large elevation angles.

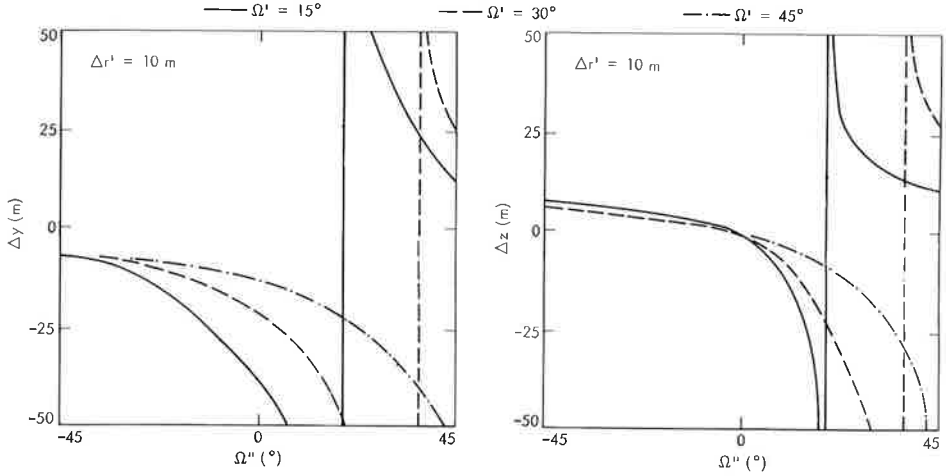

Fig. 5. Examples of error curves for stereo-radargrammetry.

Experimental stereo analyses have been performed by a number of authors. An overview of the results is given as Table IV. In some cases the accuracies quoted are optimistic, particularly if they concern opposite-side stereo configurations. Opposite-side stereoscopic viewing may be mainly possible in the case of fairly flat terrain or only isolated mountains surrounded by flat terrain. In other cases, lay-over, shadowing, and general differences in the contents of overlapping image pairs may perhaps not permit opposite-side stereo measurements to be taken, although geometrically, the opposite-side stereo arrangement is certainly superior.

The two results marked by an asterisk (*) deserve special comments: Goodyear (1974) measured a single profile of 6 km length and used one control point for "absolute orientation." The results are therefore not really comparable to those of other authors (Goodyear's control density: 1 point per $3 \times 3 \times \pi \approx 30$ km^2 corresponds to ~ 3 points per 100 km^2). The other comment pertains to the results of Leberl (1975e) using lunar orbital radar: here, a 2 m radar wavelength, very steep look-angles and not very well identifiable surface features (craters) were employed. As a result, the accuracy achieved had to be somewhat less than in studies with airborne radar. The lunar mapping study provided evidence that the stereo-radar computation according to eq. 16 is superior to eq. 18.

Contouring

Contouring from radar stereo models has been reported on two occasions: Norvelle (1972) demonstrated the use of the analytical plotter AS-11-A to directly plot contour lines from a deformed radar model. Leberl (1975e)

TABLE IV

Mapping accuracy achieved by stereo-radargrammetry

SOURCE	YEAR	ACCURACY (Meters)			CONTROL per 100 km^2	RESOLUTION (Ground -) Meters	ANTENNA		RADAR System Code	REMARKS
		along 1σ	across 1σ	height 1σ			Stabilized	Type		
Gracie	1970	12.2	7.7	13.2	35.0	17	yes	synth.	AN-APQ 102	Opp. Side
Konecny	1972	68.0	138.0	240.0		17	yes	real	Westinghouse	Opp. Side
		130.0	428.0	1548.0						Same Side
DBA-Systems	1974	26.8	21.9	16.7	1.2	3	yes	synth.	AN-ASQ142	Opp. Side
		29.5	25.6	19.7						Same Side
Goodyear	1974			93.0	3.3	12	yes	synth.	GEMS 1000	Same Side
Derenyi	1975			33.0		12	yes	synth.	GEMS 1000	Opp. Side
				177.0						Same Side
Leberl	1975	173.0	510.0	109.0	0.3	30-150	no	synth.	Apollo 17	Same Side - Small Base - Satellite

produced a radar contour plot of a lunar feature, however not by directly tracing the contour lines, but by first acquiring a digital height model, from which the contours were interpolated numerically.

MAPPING FROM BLOCKS OF OVERLAPPING IMAGERY

General

Investigations into the three-dimensional adjustment of a radar block have been reported by DBA-Systems (1974) and Dowideit (1975). A review of methods of sequential and simultaneous adjustment of original radar strips and of independent stereo models has been compiled by Leberl (1976b). However, these studies mainly concern the mathematical and statistical formulation of a solution to the problem. Actual computations concern themselves in the case of Dowideit (1975) with only a single simulated stereo pair, and in the case of DBA-Systems (1974) with a triplet of actual radar images. The modesty of the past efforts in this field could in part be caused by a certain lack of prospective block adjustment applications.

Applications exist, however, for the preparation of base maps for radar mosaicking of large numbers or radar strips. Consequently, a number of results are available on the accuracy of purely planimetric adjustments of radar strips (Berlin, 1971; Van Roessel and De Godoy, 1974; Leberl, 1975c,d).

Planimetric adjustment of overlapping radar strips

Computation of ground coordinates from a block of overlapping side-looking radar images in a process similar to photogrammetric strip adjustment was attempted first by Bosman et al. (1972b) but with a block of only two radar strips. The first adjustment of an extensive block of overlapping radar strips to a set of control points had to be made in the framework of an operational radar mapping project — PRORADAM of Colombia (Leberl, 1975c This was followed by a numerical simulation experiment — as an afterthought to the actual operational task (Leberl, 1975d). Most recently an exceptional block of radar imagery of a well-mapped area in the U.S.A. (W. Virginia) required an operational adjustment, but also permitted an experiment to be carried out to study the performance of several methods (Leberl et al., 1976).

The numerical simulation study referred to above (Leberl, 1975d) did show the following: if a radar block is formed by sequential connection of the original radar strips (or stereomodels) whereby spline functions are used to describe image deformations, and if then an external block adjustment, according to Schut (1970), is carried out then results are obtained that compare favorably with simultaneous planimetric adjustments. The sequential method is very simple, fast and numerically stable. The simultaneous methods are expensive, slow and numerically unstable.

Fig. 6 illustrates the results achieved in sequential adjustment of actual radar

blocks PRORADAM and West Virginia to sets of ground control points. It appears that with a density of ground control of about 15 points per 100 000 km^2, point accuracies achieved are about ±150 m.

Mosaicking

Mosaicking of radar strips can be carried out using the results of the numerical adjustment as a base map. However, the individual radar strips cannot be rectified, except for elimination of scale differences along- and across-track. Therefore, one must expect that mosaicking itself contributes a sizeable mapping error, even if the results of the numerical adjustment were entirely error-free.

In the case of the block West Virginia, check and ground-control points were scaled off the mosaics at a scale of 1:250,000 and off the topographic maps at 1:24,000, using in both cases the grids printed on the map sheets. It was found that both groups of points had the same errors of approximately ±200 m. This shows that the mosaicking of largely unrectified radar images added an error that obscures the errors of the numerical adjustment (±130 m).

Other methods of mosaicking have been and are in use. A method applied in the initial phase of Brazil's project RADAM is based on complete SHORAN tracking of all mapping flights. An ordered set of image points is then transformed onto a base using the measured aircraft positions and image ground ranges. The images are laid out on this base. This results in mosaics with r.m.s. errors of about ±300 m (Van Roessel and De Godoy, 1974).

In most of the enormous RADAM project of Brazil (9 million km^2), howeve not all of the mapping flights were SHORAN controlled; in fact, none of the production flights were controlled, and only a small number of transverse cross

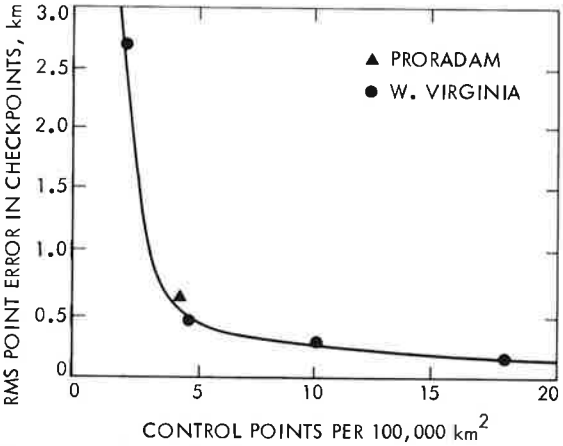

Fig. 6. Control point density and accuracy of planimetric adjustment of overlapping radar images; obtained from operational radar mapping projects: PRORADAM (Colombia) and West Virginia.

lines (tie-lines) were. Mosaics were laid out using the SHORAN controlled tie-lines as a geometric reference. This method of mosaicking was estimated by Van Roessel and De Godoy (1974) to lead to errors of the order of magnitude of ±700 m.

It is thus obvious that mosaics based on a numerical planimetric adjustment are more accurate than those resulting from other methods. It can even be expected that the numerical approach is the least expensive one (Leberl, Jensen et al., 1976).

Three-dimensional adjustment of radar blocks

The only 3-D block adjustment with actual radar imagery so far has been reported by DBA-Systems (1974)*. In this adjustment the flight data are described by spline functions of time t. The coefficients of the splines are solved in the simultaneous adjustment, based on the linearized projection eqs. 6, 7. Also the measurements of slant range and time are being calibrated in the simultaneous adjustment by postulating an error behaviour according to polynomials:

$$\begin{aligned} t + v_t &= t_0 + a_1 r^2 + a_3 r^3 \\ r + v_r &= r_0 + b_1 + b_2 r + b_3 r^2 \end{aligned} \qquad (21)$$

t, r are observations, v_t, v_r are corrections, $t_0\, r_0$ are approximations, and a_1, . . . ,b_3 unknown. The program employed by DBA-Systems is thus similarly general as are the well-known photogrammetric bundle adjustment programmes with additional parameters.

Table V reviews the results obtained by DBA (1974) with a block of three radar images. Use was made of interferometer measurements in the single-image approach and of HIRAN tracking of the aircraft.

The very interesting result of Table V is that even same-side stereo provides higher accuracy than use of the interferometer in conjunction with a single image. The study by DBA-Systems (1974) also indicated that inclusion of interferometer data in the stereo or triplet intersection does not improve the results.

CONCLUSIONS — RECOMMENDATIONS

Review of present status

The period since 1972 has, for radargrammetry, been marked by the declassification of military know-how (studies and 3 × 3 m² resolution imagery), extensive operational reconnaissance-type mapping projects (mainly Latin

*At the recent ISP-Congress, Dowideit presented results of a 3-D radar block adjustment using four image strips (Dowideit, 1976 " A Block Adjustment for SLAR-Imagery": Pres. Paper, Comm. III).

lines (tie-lines) were. Mosaics were laid out using the SHORAN controlled tie-lines as a geometric reference. This method of mosaicking was estimated by Van Roessel and De Godoy (1974) to lead to errors of the order of magnitude of ±700 m.

It is thus obvious that mosaics based on a numerical planimetric adjustment are more accurate than those resulting from other methods. It can even be expected that the numerical approach is the least expensive one (Leberl, Jensen et al., 1976).

Three-dimensional adjustment of radar blocks

The only 3-D block adjustment with actual radar imagery so far has been reported by DBA-Systems (1974)*. In this adjustment the flight data are described by spline functions of time t. The coefficients of the splines are solved in the simultaneous adjustment, based on the linearized projection eqs. 6, 7. Also the measurements of slant range and time are being calibrated in the simultaneous adjustment by postulating an error behaviour according to polynomials:

$$\begin{aligned} t + v_t &= t_0 + a_1 r^2 + a_3 r^3 \\ r + v_r &= r_0 + b_1 + b_2 r + b_3 r^2 \end{aligned} \qquad (21)$$

t, r are observations, v_t, v_r are corrections, $t_0 r_0$ are approximations, and a_1, . . . ,b_3 unknown. The program employed by DBA-Systems is thus similarly general as are the well-known photogrammetric bundle adjustment programmes with additional parameters.

Table V reviews the results obtained by DBA (1974) with a block of three radar images. Use was made of interferometer measurements in the single-image approach and of HIRAN tracking of the aircraft.

The very interesting result of Table V is that even same-side stereo provides higher accuracy than use of the interferometer in conjunction with a single image. The study by DBA-Systems (1974) also indicated that inclusion of interferometer data in the stereo or triplet intersection does not improve the results.

CONCLUSIONS — RECOMMENDATIONS

Review of present status

The period since 1972 has, for radargrammetry, been marked by the declassification of military know-how (studies and 3 × 3 m² resolution imagery), extensive operational reconnaissance-type mapping projects (mainly Latin

*At the recent ISP-Congress, Dowideit presented results of a 3-D radar block adjustment using four image strips (Dowideit, 1976 " A Block Adjustment for SLAR-Imagery": Pres. Paper, Comm. III).

a result that could perhaps not hold up outside the laboratory environment, but that should warrant more attention for stereo radar than has been given in the context of reconnaissance-type radar-mapping projects.

Radar block adjustment is a field of study that has not attracted the attention of many research workers. The comparatively weak geometry of all dynamic (kinematic) imaging systems does not present great promise for control network densification based on image blocks. However, in the context of reconnaissance-type mapping, of image mosaicking for mapping of sea and lake ice, and for future planetary exploration (mapping of the planet Venus), radar block adjustment techniques should have valuable applications.

Recommendations

Recommendations for future work on radargrammetry should be based on the present trend to view remote sensing as a tool in which various sensors are integrated into one coherent system: each sensor is producing only a specific component of data; but only the integration of all the data from various sources will allow the maximum benefit to be obtained from remote sensing. This particularly will be the case with satellite radar, to be combined with LANDSA' and similar data. In this context, the most significant tasks of radargrammetry are in relating the radar image to other remote sensing data sources. Solution of these problems will call for differential rectification or digital monoplotting, employing perhaps the techniques of digital image processing.

Application of radar to classical mapping tasks has limited itself to reconnaissance-type mapping of remote areas. It is felt that the radar images have not been used to their full potential in these projects. It is thus recommend ed to apply more radargrammetric expertise in radar mapping projects, so that advantage is taken of the metric information potential of imaging radar.

Apart from reconnaissance-type mapping, radar might also have some potential as a tool for map revision. Particularly the advent of satellite radar may suggest exploration of the limits and possibilities of radar map revision.

Stereo radargrammetric analyses have in the past not dealt with the rather important relationships that exist between physiological limits to perceiving and measuring a radar stereo model and various parameters of the radar configuration and of the imaged area. Such an analysis, while pertinent to stereo radargrammetry, would generate results of significance far outside the mapping community.

New mapping tasks which have not existed in the past but are becoming significant now and can be solved by radar, address the mapping of sea and lake ice, and perhaps of cloud covered planetary surfaces such as Venus. The next few years might see ice mapping as a major radargrammetric task, while planetary exploration by radar images is in the more distant future.

ACKNOWLEDGEMENT

I wish to express my gratitude to Dr. Ch. Elachi, D. Baker, V. Arriola and E. Abbott for their support during the preparation of this paper.

REFERENCES

Akowetzki, W.I., 1968. On the transformation of radar coordinates into the geodetic syste Geod. Aerofotosjomka, 1968 (in Russian).

Ambrose, W., 1967. A radar image correlation viewer. Photogramm. Eng., 33.

Bair, G.L. and Carlson, G., 1975. Height measurement with stereo radar. Photogramm. En Remote Sensing, 41.

Bair, L.G. and Carlson, G.E., 1974. Performance comparison of techniques for obtaining stereo radar images. IEEE Trans. Geosci. Electron., GE-11.

Berlin, G.L., 1971. Radar mosaics. Prof. Geogr., 23(1).

Bicknell, T. et al., 1975. A study to determine the feasibility of using radar techniques for public land surveying. Jet Propulsion Laboratory Report under contract to the Bureau of Land Management, Contract No. 53500-PH3-995, Pasadena, Calif.

Bosman, E. et al., 1971. Project Karaka — The transformation of points from side looking radar images into the map system. Final Report, Part 1, Netherlands Interdepartmental Working Community for the Application and Research of Remote Sensing Techniques (NIWARS), Delft.

Bosman, E.R., Clerici, E., Eckhart, D. and Kubik, K., (undated). Project BEBLOKA — The transformation of points from overlapping images obtained with different sensors into the map system. Final Report, Netherlands Interdepartmental Working Community for the Application and Research of Remote Sensing Techniques (NIWARS), Delft.

Bosman, E.R., Clerici, E., Eckhart, D. and Kubik, K., 1972a. Transformation of points from side-looking radar images into the map system. Bildmessung Luftbildwesen, 42(2)

Bosman, E.R., Clerici, E., Eckhart, D. and Kubik, K., 1972b. KARIN — A program system for the mapping of remote sensing information. Pres. Pap., 12th Congr. Int. Soc. Photogrammetry, Ottawa; also Final Report, Netherlands Interdepartmental Working Community for the Application and Research of Remote Sensing Techniques (NIWARS Delft.

Carlson, G.E., 1973. An improved single flight technique for radar stereo. IEEE Trans. Geosci. Electron., GE-11(4).

Claveloux, B.A., 1960. Sketching projector for side looking radar photography. Photogram Eng., 26.

Cohen, E. et al., 1975. An earth and ocean SAR for space shuttle-user requirements and data handling implications. Proc. Natl. Telecomm. Conf., New Orleans, La.

Crandall, C.J., 1963. Advanced radar map compilation equipment. Photogramm. Eng., 29.

Crandall, C.J., 1969. Radar mapping in Panama. Photogramm. Eng., 35.

Dalke, G. et al., 1968. Regional slopes with non stereo radar. Photogramm. Eng., 34.

DBA Systems, 1974. Research studies and investigations for radar control extensions. DBA Systems Inc., Melbourne, Fla. (Defense Documentation Center Report No. 53078

De Azevedo, L., 1971. Radar in the Amazon. Proc. 7th Int. Symp. Remote Sensing of the Environment. Ann Arbor, Mich.

Derenyi, E.E., 1970. An Exploratory Investigation into the Relative Orientation of Continuous Strip Imagery. Thesis and Research Report No. 8, Univ. of New Brunswick, Fredericton, N.B.

Derenyi, E.E., 1972. Geometric considerations in remote sensing. Proc. 1st Canadian Symp on Remote Sensing. Ottawa.

Derenyi, E.E., 1974a. SLAR geometric test. Photogramm. Eng., 40.
Derenyi, E.E., 1974b. Metric evaluation of radar and infrared imageries. Proc. 2nd Canadia Symp. on Remote Sensing. Univ. of Guelph, Guelph, Ont.
Derenyi, E.E., 1975a. Topographic accuracy of side looking radar imagery. Bildmessung Luftbildwesen, 1975(1).
Derenyi, E.E., 1975b. Terrain heights from SLAR Imagery. Pres. Pap. 41st Annual Conv. Am. Soc. Photogramm., Washington, D.C.
DiCarlo, C. et al., 1968. All weather mapping. Pres. Pap. Int. Congr. of Surveyors (FIG), London.
DiCarlo, C. et al., 1971. DoD data processing equipment for radar imagery. Pres. Pap. Int. Congr. of Surveyors, Wiesbaden.
Dowideit, G., 1975. A simulation system for theoretical analysis of radar restitution and a test by adjustment. Proc. Symp. Comm. III, Int. Soc. Photogramm., Stuttgart. In: Deutsche Geodätische Kommission, Reihe B, Heft No. 214.
Egbert, E., 1969. Calculation of ground street lengths and area from radar measurements. In: D.S. Simonnett (Editor), The Utility of Radar and Other Remote Sensors in Themat Land Use Mapping from Spacecraft. Annu. Rep. U.S. Geol. Surv., Interagency Report-NASA 140.
Esten, R.D., 1953. Radar relief displacement and radar parallax. USAERDL-Report No. 1294, Ft. Belvoir, Va.
Fiore, C., 1967. Side looking radar restitution, Photogramm. Eng., 33.
Geier, F., 1971. Beitrag zur Geometrie des Radarbildes. Thesis, Techn. Univ., Graz (in German).
Geier, F., 1972. Fundamentals of orientation for radar PPI images with approximated horizontal distances. Pres. Pap., 12th Congr., Int. Soc. Photogramm., Ottawa.
Glushkov, W.M. et al., 1972. Toros — Side looking radar system and its application for sea ice condition study and for geologic explorations. Pres. Pap., 12th Congr., Int. Soc. Photogramm., Ottawa.
Goodyear, 1972. Flight test report all-weather topographic mapping system AN/ASQ-142. Contract No. F 33657-70-C-0769, Goodyear Aerospace Corp., Litchfield Park, Ariz.
Goodyear, 1974. Preliminary imagery data analysis Goodyear Electronic Mapping System (GEMS). Goodyear Aerospace Corp., Report GIB-9342, Code 99696.
Gracie, G. et al., 1970. Stereo radar analysis. U.S. Eng. Topogr. Lab., Ft. Belvoir, Va., Report No. FTR-1339-1.
Gracie, G. and Sewell, E.D., 1972. The Metric Quality of Stereo Radar Proc. of the Techn. Program, Electro-Optical Systems Design Conference, New York, 12—14 Sept.
Graham, L.C., 1970. Cartographic applications of synthetic aperture radar. Proc. Am. Soc. Photogramm., 37th Annual Meeting; and Goodyear Aerospace Corp., Report GERA-1626.
Graham, L., 1972. An improved orthographic radar restitutor. Pres. Pap., 12th Congr., Int. Soc. Photogramm., Ottawa; also in Goodyear Aerospace Corp., Report GERA-1831.
Graham, L. and Rydstrom, H.O., 1974. Synthetic aperture radar applications to earth resources development. Goodyear Aerospace Corp., Report GERA-2010, Code 99696.
Graham, L.C., 1975a. Geometric problems in side-looking radar imaging. Proc. Symp. Comm. III, Int. Soc. Photogramm.; Stuttgart, W. Germany; In: Deutsche Geodätische Kommission, Reihe B, Heft No. 214.
Graham, L., 1975b. Flight planning for stereo radar mapping. Proc. Am. Soc. Photogramm., 41st Meet., Washington, D.C.
Greve, C. and Cooney, W., 1974. The digital rectification of side looking radar. Proc. Am. Soc. Photogramm., Annu. Conv., Wash., D.C.
Hall, D., 1973. Digital cartographic compilation. In: A Compendium of Techn. Papers on Experiments in Cartography at Rome Air Development Center. Pres. Pap. Pan Am. Inst. Geogr. Hist., Panama, by Air Force Systems Command, Rome Air Development Center, Griffiss Air Force Base, N.Y.

Harris, G. and Graham, L.C., 1976. LANDSAT — radar synergism. Pres. Pap., 13th Int. Congr. Soc. Photogramm., Comm. VII, Helsinki.

Hirsch, Th. and Van Kuilenburg, J., 1976. Preliminary tests of the EMI-SLAR mapping quality. Netherlands Interdepartmental Working Community for the Appli. and Res. of Remote Sensing (NIWARS), Internal Report No. 39, Delft.

Hockeborn, H.A., 1971. Extraction of positional information from side looking radar. Bildmessung Luftbildwesen, 39(1).

Hoffmann, P., 1958. Photogrammetric applications of radar scope photographs. Photogramm Eng., 24.

Hohenberg, F., 1950. Zur Geometrie des Funkmessbildes. Austrian Academy of Sciences, Math.-Naturwissenschaftliche Klasse, Vienna, Vol. 2—3.

Jensen, H., 1972. Mapping with coherent-radiation focused synthetic aperture side-looking radar. In: Operational Remote Sensing: An Interactive Seminar to Evaluate Current Capabilities. Am. Soc. Photogramm.

Jensen, H., 1975. Deformations of SLAR imagery-results from actual surveys. Proc. Symp. Comm. III, Int. Soc. Photogramm., Stuttgart. In: Deutsche Geodätische Kommission, Reihe B, Heft No. 214.

Kober, C.L. et al., 1950. Determination of target height from radar PPI-Photographs. Air Force Tech. Rep. No. 6500, Wright Air Development Center, Ohio.

Konecny, G. and Derenyi, E.E., 1966. Geometric considerations for mapping from scan imagery. Proc. 4th Symp. Remote Sensing of the Environment, Ann Arbor, Mich.

Konecny, G., 1970. Metric problems in remote sensing. Publications of the International Institute for Aerial Surveying and Earth Sciences (ITC), Delft, Series A, No. 50.

Konecny, G., 1971. Orientierungsfragen bei Streifenbildern und Aufnahmen der Infrarot-abtastung. Bildmessung Luftbildwesen, 41(1).

Konecny, G., 1972a. Geometrical aspects of remote sensing. Arch. Int. Soc. Photogramm., Invited Paper, 12th Congr., Ottawa.

Konecny, G., 1972b. Geometrische Probleme der Fernerkundung. Bildmessung Luftbildwese 42(2).

Konecny, G., 1975. Approach and status of geometric restitution for remote sensing imagery Proc. Symp. Comm. III, Int. Soc. Photogramm., Stuttgart; In: Deutsche Geodätische Kommission, Reihe B, Heft No. 214.

Koopmans, B., 1974. Should stereo SLAR imagery be preferred to single strip imagery for thematic mapping? ITC-Journal 1974-3, Enschede.

Korneev, I.U.N., 1975. Analytical method for photogrammetric processing of a single radar photograph. Geod. Aerofotosjomka, 1975(2) (in Russian).

LaPrade, G.L., 1963. An analytical and experimental study of stereo for radar. Photogramm. Eng., 29.

LaPrade, G.L. et al., 1969. Elevations from radar imagery. Photogramm. Eng., 35.

LaPrade, G.L., 1970. Subjective considerations for stereo radar. Goodyear Aerospace Corp., Report GIB-9169, and Photogramm. Eng.

LaPrade, G.L., 1975. Radar signature of inverted catenary with equilateral triangular cross section (St. Louis Gateway Arch). Arizona Electronics Eng. Memo. No. 525, Goodyear Aerospace Coop., Arizona Div., Litchfield Park, Ariz.

Leberl, F., 1970. Metric properties of imagery produced by side looking airborne radar and infrared line scan systems. Publications of the International Institute for Aerial Survey and Earth Sciences (ITC), Series A, No. 50, Delft.

Leberl, F., 1971a. Vorschläge zur instrumentellen Entzerrung von Abbildungen mit Seitwärts Radar (SLAR) und Infrarotabtastsystemen. Bildmessung Luftbildwesen, 39.

Leberl, F., 1971b. Remote Sensing — Neue Methoden zur Wahrnehmung auf Abstand. Osterreichische Zeitschrift für Vermessungswesen, No. 6.

Leberl, F., 1971c. Untersuchung über die Geometrie und Einzelbildauswertung von Radar-schrägaufnahmen. Thesis, Tech. Univ., Vienna.

Leberl, F., 1972a. Evaluation of single strips of side looking radar imagery. Arch. Int. Soc. Photogrammetry, Invited Pap., 12th Congr., Ottawa.
Leberl., F., 1972b. On model formation with remote sensing imagery. Österreichische Zeitschrift für Vermessungswesen No. 2.
Leberl, F., 1972c. Radargrammetria para los Interpretes de Imagenes Centro Interamericano de Fotointerpretacion, (CIAF), Bogota, Colombia.
Leberl, F., 1974. Evaluation of SLAR Image Quality and Geometry for PRORADAM. ITC-Journal, 2(4).
Leberl, F., 1975a. The geometry of, and plotting from, single strips of side looking airborne radar imagery. International Institute for Aerial Survey and Earth Sciences (ITC) Technical Report No. 1, Enschede.
Leberl, F., 1975b. Radargrammetry for Image Interpreters, ITC Tech. Rep. No. 2, Enschede
Leberl, F., 1975c. Radargrammetric point determination PRORADAM. Bildmessung Luftbildwesen, 45(1).
Leberl, F., 1975d. Sequential and simultaneous SLAR block adjustment. Photogrammetria, 31(1).
Leberl, F., 1975e. Lunar Radargrammetry with ALSE-VHF Imagery. Proc. Am. Soc. Photogramm., Fall Tech. Meeting, Phoenix, Ariz.
Leberl, F., 1976a. Mapping of lunar surface from side-looking orbital radar images. The Moon, in press.
Leberl, F., 1976b. Satelliten-Radargrammetrie. Dtsch. Geod. Komm., Reihe C, in press.
Leberl, F., Farr, T., Bryan, L. and Elachi, C., 1976a. Study of Arctic Sea Ice Drift from L-Band Side Looking Radar Imagery. Proc. Am. Soc. Photogramm., 42nd Ann. Conv., Washington, D.C.
Leberl, F., Jensen, H. and Kaplan, J., 1976b. Side-looking radar mosaicking experiment. Photogramm. Eng. and Remote Sensing, 42.
Leonardo, E., 1959. An application of photogrammetry to radar research. Photogramm. Eng., 25.
Leonardo, E., 1963. Comparison of imaging geometry for radar and photographs. Photogramm. Eng., 29.
Leonardo, E., 1964. Capabilities and limitations of remote sensors. Photogramm. Eng., 30.
Levine, D., 1960. Radargrammetry. McGraw-Hill, New York, N.Y.
Levine, D., 1963. Principles of stereoscopic instrumentation for PPI-photographs. Photogramm. Eng., 30.
Levine, G., 1965. Automatic production of contour maps from radar interferometric data. Pres. Pap., Fall Tech. Meet., Am. Soc. Photogramm., Dayton, Ohio.
Lewis, A.J. and MacDonald, H.C., 1970. Interpretive and Mosaicking Problems of SLAR Imagery. Remote Sensing Environ., 1(4).
Loelkes, G.L., 1965. Radar mapping imagery — Its enhancements and extraction for map construction. Pres. Pap., Fall Tech. Meet., Am. Soc. Photogramm., Dayton, Ohio.
Luchininov, V.S., 1975. Contactless radar mapping of warm valley glaciers — Transformation of radar coordinates. Transl. from Russian in Sov. Phys. Tech. Phys., 20(4).
Macchia, R.P., 1957. Radar presentation restitutor. Photogramm. Eng., 23.
Makarovic, B., 1973. Digital monoplotters. ITC-Journal, 1973-4, Enschede.
Manual of Photogrammetry, 1966. Photogrammetric and Radargrammetric Techniques, II, 3rd ed.
Masry, S.E., 1969. Analytical treatment of stereo strip photos. Photogramm. Eng., 35.
Masry, S.E., Derenyi, E.E. and Crawley, B.G., 1976. Photomaps from non-conventional imagery. Photogramm. Eng. Remote Sensing, 42(4).
Miranda, A., 1970. Radar stereo equipment. Goodyear Aerospace Corporation, Report GIB-9198.
Moore, R.K., 1969. Heights from simultaneous radar and infrared. Photogramm. Eng., 35.

Moreira, H.F., 1973. Project RADAM — Remote sensing application to environment analysis of Amazon region. 2nd Annual Remote Sensing of Earth Resources Conference, Univ. of Tennessee Space Inst., Tullahoma, Tennessee.

Norvelle, F.R., 1972. AS-11-A Radar Program. Photogramm. Eng., 38.

Peterson, R.K., 1976. The correction of anamorphic scale errors in holographic radar imagery Goodyear Aerospace Report, Code 99696, Litchfield Park, Ariz., Pres. Pap., 13th Congr. Int. Soc. Photogramm., Helsinki.

Phillips, R. et al., 1973. Apollo lunar sounder experiment. Apollo-17 Preliminary Science Report, NASA-SP 330, Washington, D.C.

Protherse, W.M. et al., 1950. The geometry of the radarscope. Tech. Paper, No. 107, Mapping and Charting Laboratory, Ohio State Univ., Ohio.

Raytheon Co., 1973. Digital rectification of side-looking radar (DRESLR). Final Report, Raytheon Co., Autometric Operation, Prep. for U.S. Army Engineer Topographic Laboratories, Fort Belvoir, Va., 22060, Rep. No. ETL-CR-73-18.

Rinner, K., 1948. Die Geometrie des Funkmessbildes. Austrian Academy of Sciences, Math. Naturwiss. Klasse; also in: Handbuch der Vermessungskunde. Jordan-Eggert-Kneissl, Vol. VI, Metzlersche Verlagsbuchhandlung, Stuttgart, 1966.

Roessel, J. van and De Godoy, R., 1974. SLAR mosaics for Project RADAM. Photogramm. Eng., 40.

Rose, J. and Friedman, L., 1974. A design for a Venus orbital imaging radar mission. Am. Inst. Aeronaut. Astronaut., AIAA-Pap. No. 74-222.

Rosenfield, G.H., 1968. Stereo Radar Techniques. Photogramm. Eng., 34.

Rydstrom, H.C., 1968. Radargrammetric Applications of the Right Angle Solution Nomogra Goodyear Aerospace Corp., Report GIB 9124, Litchfield Park, Ariz.

Scheps, B.B., 1960. To Measure is to know — Geometric fidelity and interpretation in radar mapping. Photogramm. Eng., 26.

Schertler, R.J. et al., 1975. Great Lakes all-weather ice information system. Proc. 10th Symp Remote Sensing of the Environment, Ann Arbor, Mich.

Schreiter, J.B., 1950. Strip projection for radar charting. Tech. Paper No. 130, Mapping and Charting Laboratory, Ohio State Univ., Ohio.

Schut, G., 1970. External block adjustment of planimetry. Photogramm. Eng., 36(9).

Smith, H.P., 1948. Mapping by radar — The Procedures and possibilities of a new and revolutionary method of mapping and charting. U.S. Air Force, Randolph Field, Texas.

Stilwell, J.E., 1963. Radar network adjustment. Photogramm. Eng., 29.

Super, A.D. et al., 1975. Remote sensing applied to the international ice patrol. Proc. 10th Symp. on Remote Sensing of the Environment, Ann Arbor, Mich.

Tiernan, M. et al., 1976. Lunar Cartography with the Apollo 17 ALSE Radar Imagery. The Moon, 15(1/2).

Thomann, G.C., 1969. Acoustic simulation of stereo radar. Tech. Mem. No. 133-8, CRES, Univ. of Kansas, Lawrence, Kansas.

Thomann, G., 1969. Distance computation on radar film. In: D.G. Simonnett (Editor), The Utility of Radar and Other Remote Sensors in Thematic Land Use Mapping from Spacecraft. Annu. Rep., U.S. Geol. Surv., Interagency Report, NASA-140.

Thompson, T.W. et al., 1972. Progress report on 25cm radar observations of the 1971 AIDJEX studies. Arctic Ice Dynamics Joint Experiment (AIDJEX) Bulletin, No. 12, Univ. of Wash., Seattle, Wash.

Yoritomo, K., 1965. All weather mapping. Pres. Pap., Fall Tech. Meet., Soc. Photogramm., Dayton, Ohio.

Yoritomo, K., 1972. Methods and instruments for the restitution of radar pictures. Arch. Int. Soc. Photogramm., Inv. Pap., 12th Congr., Ottawa.